White Rose Research Online

eprints@whiterose.ac.uk
https://eprints.whiterose.ac.uk
Universities of Leeds, Sheffield and York

Deposited via The University of Sheffield.

White Rose Research Online URL for this paper:
https://eprints.whiterose.ac.uk/id/eprint/180861/

Version: Published Version

Article:

Luo, P, Madathil, S, Saito, W. et al. (2022) Investigation of turn-on performance in 1.2 kV MOS-bipolar devices. Japanese Journal of Applied Physics, 61 (SC). SC0801. ISSN: 0021-4922

https://doi.org/10.35848/1347-4065/ac40aa

Reuse
This article is distributed under the terms of the Creative Commons Attribution (CC BY) licence. This licence allows you to distribute, remix, tweak, and build upon the work, even commercially, as long as you credit the authors for the original work. More information and the full terms of the licence here: https://creativecommons.org/licenses/

Takedown
If you consider content in White Rose Research Online to be in breach of UK law, please notify us by emailing eprints@whiterose.ac.uk including the URL of the record and the reason for the withdrawal request.

UNIVERSITY OF LEEDS University of Sheffield UNIVERSITY of York

Japanese Journal of Applied Physics

The Japan Society of Applied Physics

PROGRESS REVIEW • OPEN ACCESS

Investigation of turn-on performance in 1.2 kV MOS-bipolar devices

To cite this article: Peng Luo *et al* 2022 *Jpn. J. Appl. Phys.* **61** SC0801

View the article online for updates and enhancements.

You may also like

- Simulation study on a novel snapback-free and low turn-off loss reverse-conducting SOI-LIGBT with P-type double trench gates on the anode region
Bingke Zhang, Moufu Kong, Bo Yi et al.

- Simulation study of a novel thin layer SOI carrier-stored TLIGBT with self-biased pMOS
Bo Yi, Jia Lin, Huan Hu et al.

- Research on Parallel Operation Characteristics and Current Sharing Method of High Power IGBT
Tang Yong, Wang Bo and Lin Qiu Jie

This content was downloaded from IP address 143.167.254.164 on 01/03/2022 at 13:55

OPEN ACCESS

Japanese Journal of Applied Physics **61**, SC0801 (2022) **PROGRESS REVIEW**

https://doi.org/10.35848/1347-4065/ac40aa

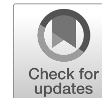

Investigation of turn-on performance in 1.2 kV MOS-bipolar devices

Peng Luo[1*], Sankara Narayanan Ekkanath Madathil[1], Wataru Saito[2], and Shin-ichi Nishizawa[2]

[1]*Department of Electronic and Electrical Engineering, The University of Sheffield, United Kingdom*
[2]*Research Institute for Applied Mechanics, Kyushu University, Japan*

[*]E-mail: peng.luo@sheffield.ac.uk

Received September 29, 2021; revised November 20, 2021; accepted December 7, 2021; published online February 21, 2022

In this paper, the turn-on characteristics of the 1.2 kV Trench IGBT (TIGBT) and the 1.2 kV Trench Clustered IGBT (TCIGBT) are investigated through TCAD simulations and experiments. The TCIGBT shows much lower turn-on energy loss (E_{on}) due to higher current gain than an equivalent TIGBT and the negative gate capacitance effect is effectively suppressed in the TCIGBT by its self-clamping feature and PMOS action. In addition, the impact of 3D scaling rules on the turn-on performance of TIGBT and TCIGBT is analyzed in detail. Simulation results show that scaling rules result in a significant reduction of E_{on} in both TIGBT and TCIGBT. Furthermore, the experimental results indicate that TCIGBT technology is well suited for high current density operations with low power losses. Compared to the state-of-the-art IGBT technology, an 18% reduction of total power loss can be achieved by the TCIGBT operated at 300 A cm^{-2} and 175 °C. © 2022 The Author(s). Published on behalf of The Japan Society of Applied Physics by IOP Publishing Ltd

1. Introduction

The trends in the development of silicon MOS-bipolar devices have always been devoted to continuous increases in power density as well as power efficiency. Remarkable efforts have been made to improve the turn-off energy loss (E_{off}) versus on-state voltage drop ($V_{ce(sat)}$) trade-off. For example, the 3D scaling concepts on trench IGBT (TIGBT)[1–3] and trench clustered IGBT (TCIGBT)[4] have resulted in significant improvements in E_{off}–$V_{ce(sat)}$ trade-off. Due to the enhanced thyristor effect, the scaled TCIGBTs show even lower $V_{ce(sat)}$ than the scaled TIGBTs.[4] Recently, it was revealed that the dynamic avalanche (DA) phenomenon posed fundamental limits on the operating current density, turn-off energy loss, *dV/dt* controllability and long-term reliability of TIGBTs.[5–8] In comparison, the TCIGBTs have been experimentally evaluated to show DA free behavior and low power losses at high current density operations.[9–11] In addition to the on-state and turn-off behavior, the turn-on performance is also important for MOS-gated bipolar devices to achieve high switching frequency operations with low power losses.

To lower the turn-on power dissipation (E_{on}) of TIGBTs, one common method is to reduce the gate resistance (R_g) to speed up the switching transients. However, the reduction of R_g is limited by the turn-off behavior because small R_g can result in additional turn-off energy losses due to DA.[6,9] Another method to lower the E_{on} is to improve the turn-on dV_{ce}/dt by reducing the Miller capacitance (C_{gc}), such as side-gate design,[12] split-gate design[13] and adoption of emitter dummy trenches.[14,15] However, such designs may enter into "self-controlled" mode (the turn-off surge voltage is independent of R_g) if the C_{gc} is too low,[16] which limits the applications of TIGBTs. Furthermore, reducing C_{gc} also increases the turn-off *dV/dt*, which enhances the DA effect during turn-off and short-circuit conditions.[6,17] Therefore, improving the turn-on performance of TIGBTs in terms of low E_{on} and high *dV/dt* controllability by reducing C_{gc} has to be compromised with their turn-off performance. Furthermore, the negative gate capacitance (NGC) effect during the turn-on transients of IGBTs cause strong oscillations under short-circuit conditions[18] and degrade the turn-on dI_c/dt controllability, resulting in EMI noise in the applications.[19] To reduce or eliminate the EMI noise emission from IGBT modules, the NGC effect must be eliminated or suppressed without sacrificing other electrical characteristics. IGBT structures with P-float resistors[19,20] or hole path structure[21] can divert some of the holes and suppress the NGC effect, but at the cost of increased $V_{ce(sat)}$ due to weakened injection enhancement (IE) effect. Other IGBT cathode designs, such as side-gate design[12] and separate P-float design,[22] can also suppress the NGC effect by lowering the potential differences across the gate oxide. However, the impact of such designs on the turn-off behavior is not well studied.

In the previous work,[23] the turn-on behavior of 1.2 kV TIGBT and TCIGBT are studied via 3D TCAD simulations.[24] In this work, the superior turn-on performance of the 1.2 kV TCIGBT is validated through experiments. The TCIGBT shows significant improvement of E_{on} due to the inherent thyristor actions. The negative gate capacitance effect is effectively suppressed by the self-clamping feature of TCIGBT and effective PMOS action. Furthermore, the impact of 3D scaling rules on the turn-on performance of TIGBT and TCIGBT is analyzed in detail. Finally, the measured total power losses of TCIGBT are compared to the state-of-the-art IGBT technology.

2. Turn-on performance of TIGBT and TCIGBT

Figures 1(a) and 1(b) show the cross-sectional view of the 1.2 kV TIGBT and the 1.2 kV TCIGBT, respectively. Main structural parameters and threshold voltage (V_{th}), as shown in Table I, are kept identical herein to compare the turn-on performance. A double pulse inductive circuit as shown in Fig 2 is used to simulate the switching behavior. A silicon PiN diode is used as the freewheeling diode (FWD) and the current rating is set as 100 A at $J_c = 200$ A cm^{-2}. The turn-on mechanism and turn-off behavior of TCIGBT have been explained in Refs. 4 and 9. Figures 3(a) and 3(b) show the small current $I_c = 10$ A (1/10 of rated current) turn-on waveforms as a function of gate resistance (R_g) of TIGBT and TCIGBT, respectively.

Content from this work may be used under the terms of the Creative Commons Attribution 4.0 license. Any further distribution of this work must maintain attribution to the author(s) and the title of the work, journal citation and DOI.

© 2022 The Author(s). Published on behalf of The Japan Society of Applied Physics by IOP Publishing Ltd

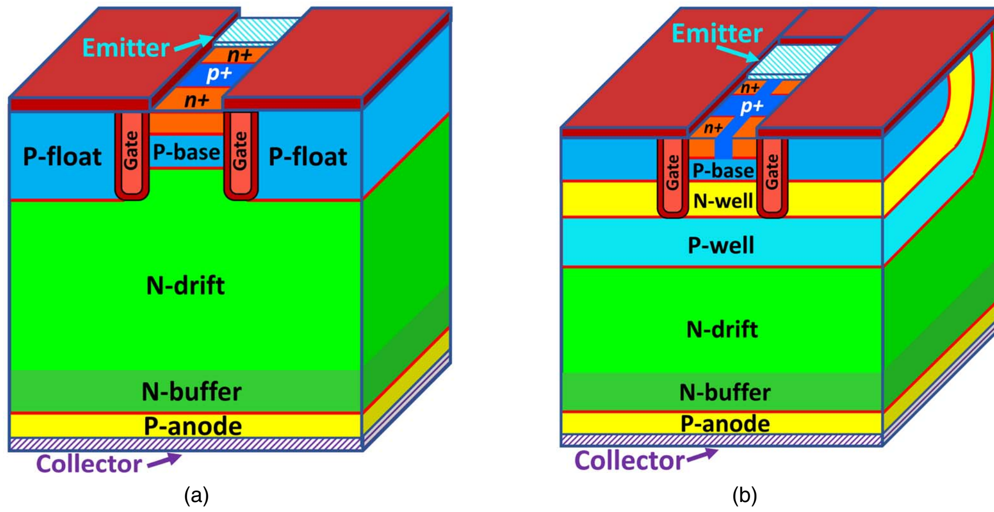

Fig. 1. (Color online) 3D cross-sectional view of (a) TIGBT and (b) TCIGBT.

Table I. Main structural parameters.

Parameters	TIGBT	TCIGBT
Device thickness	110 μm	110 μm
Cell pitch	10 μm	10 μm
Trench depth	5 μm	5 μm
Trench width	1.5 μm	1.5 μm
Mesa width	1 μm	1 μm
P-base depth	2.5 μm	2.5 μm
N-well depth	N.A.	5 μm
P-well depth	N.A.	12 μm
N-drift doping	5e13 cm^{-3}	5e13 cm^{-3}
Buffer thickness	3 μm	3 μm
Buffer doping	5e16 cm^{-3}	5e16 cm^{-3}
P-anode thickness	0.5 μm	0.5 μm
P-anode doping	1e18 cm^{-3}	1e18 cm^{-3}
Threshold voltage V_{th} (T_j = 300 K)	6 V	6 V

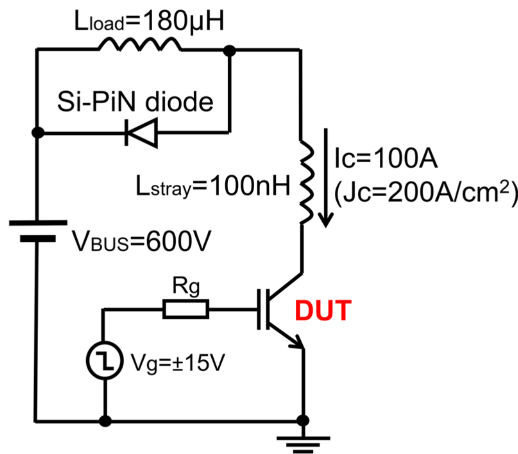

Fig. 2. (Color online) Test circuit configuration.

Figure 4 compares the turn-on waveforms at rated current I_c = 100 A and identical R_g condition. It can be seen that TCIGBT shows much higher turn-on dI_c/dt and dV_{ce}/dt than TIGBT. This is because, the thyristor structure within TCIGBT exhibits a higher current gain than the BJT structure within TIGBT, as expressed in Eqs. (1)–(4), where (1) and (2) are the turn-on dI_c/dt and dV_{ce}/dt of TIGBT, (3) and (4) are the turn-on dI_c/dt and dV_{ce}/dt of TCIGBT, g_m is the transconductance of the MOSFET structure, V_{g_in} is the gate input voltage, C_{gc} is the gate-collector capacitance, and C_{ge} is the gate-emitter capacitance.

$$\frac{dI_c}{dt} = \frac{g_m(V_{g_in} - V_{ge})}{(1-\alpha_{PNP})(R_g \times C_{ge})} \tag{1}$$

$$\left|\frac{dV_{ce}}{dt}\right| = \frac{V_{g_in} - \left(V_{th} + \frac{1-\alpha_{PNP}}{g_m} I_c\right)}{R_g \times C_{gc}} \tag{2}$$

$$\frac{dI_c}{dt} = \frac{g_m(V_{g_in} - V_{ge})}{(1-\alpha_{PNP})(1-\alpha_{NPN})(R_g \times C_{ge})} \tag{3}$$

$$\left|\frac{dV_{ce}}{dt}\right| = \frac{V_{g_in} - \left[V_{th} + \frac{(1-\alpha_{PNP})(1-\alpha_{NPN})}{g_m} I_c\right]}{R_g \times C_{gc}}. \tag{4}$$

The detailed derivation of the turn-on dI_c/dt and dV_{ce}/dt of TCIGBT can be explained as follows: the equivalent circuit model of the CIGBT[25] is essentially the use of a MOS gate structure to control a thyristor structure, which consists of a PNP transistor (P-anode/N-drift/P-well) and an NPN transistor (N-drift/P-well/N-well). During forward conduction, the MOS current serves as the base current of the PNP transistor, while the collector current of the PNP transistor serves as the base current of the NPN transistor. Therefore, the total collector/anode current follows a relationship of

$$I_c = \frac{g_m(V_{ge} - V_{th})}{(1-\alpha_{PNP})(1-\alpha_{NPN})}, \tag{5}$$

where α_{PNP} is the current gain of the PNP transistor (P-anode/N-drift/P-well), and α_{NPN} is the current gain of the NPN transistor (N-drift/P-well/N-well). By differentiating both sides of Eq. (5), it produces:

$$\frac{dI_c}{dt} = \frac{g_m}{(1-\alpha_{PNP})(1-\alpha_{NPN})} \cdot \frac{dV_{ge}}{dt}. \tag{6}$$

During the current rise phase of turn-on transient, the collector/anode voltage remains constant, and the gate current

© 2022 The Author(s). Published on behalf of
The Japan Society of Applied Physics by IOP Publishing Ltd

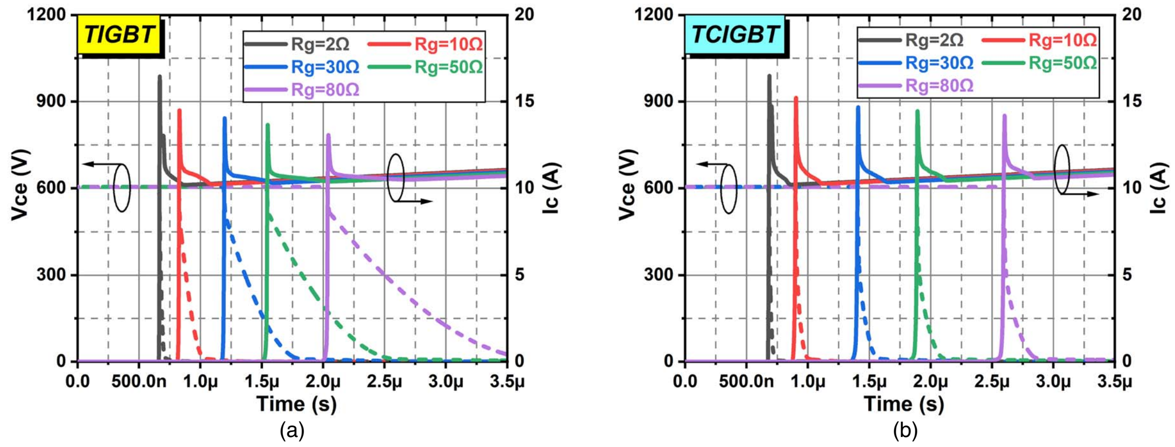

Fig. 3. (Color online) Small current turn-on performance of (a) TIGBT and (b) TCIGBT.

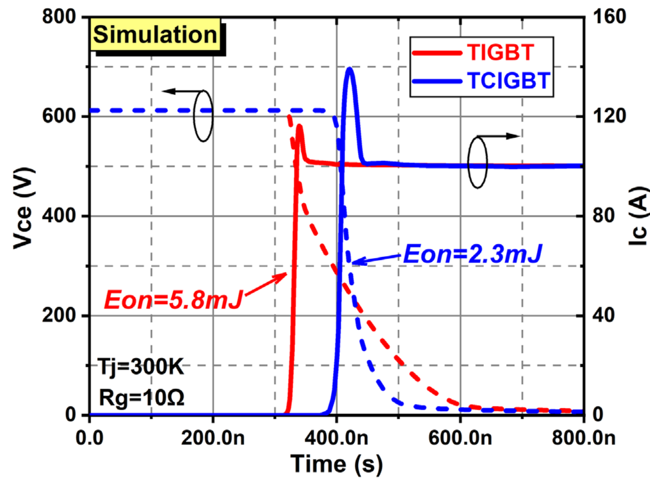

Fig. 4. (Color online) Comparison of simulated turn-on performance of TIGBT and TCIGBT at identical R_g. (TIGBT: $dI_c/dt = 7.7$ kA μs^{-1}, $dV_{ce}/dt = 2.2$ kV μs^{-1}; TCIGBT: $dI_c/dt = 11$ kA μs^{-1}, $dV_{ce}/dt = 9.4$ kV μs^{-1}).

is mainly used to charge up the C_{ge}

$$I_g = \frac{V_{g_in} - V_{ge}}{R_g} = C_{ge} \times \frac{dV_{ge}}{dt}. \tag{7}$$

Therefore, the turn-on dI_c/dt of TCIGBT can be simplified to Eq. (3).

During the collector/anode voltage fall phase, the gate voltage is fixed at the Miller plateau voltage ($V_{plateau}$). Thus, almost all the gate current is used to charge up the C_{gc} at this stage

$$I_g = \frac{V_{g_in} - V_{plateau}}{R_g} = C_{gc} \times \frac{dV_{gc}}{dt} = C_{gc} \times \frac{d(V_{ge} - V_{ce})}{dt} = C_{gc} \times \left| \frac{dV_{ce}}{dt} \right|. \tag{8}$$

If the FWD is an ideal diode with zero reverse recovery, the collector/anode current can be expressed as:

$$I_c = \frac{g_m(V_{plateau} - V_{th})}{(1 - \alpha_{PNP})(1 - \alpha_{NPN})}. \tag{9}$$

Replacing the component of $V_{plateau}$ in Eq. (8) with Eq. (9), the fall rate of the collector/anode voltage (dV_{ce}/dt) can be expressed as Eq. (4). Therefore, TCIGBT shows much lower E_{on} than the TIGBT due to higher turn-on dI_c/dt as well as higher dV_{ce}/dt. As the FWD in the case of TCIGBT experiences a higher dV_{KA}/dt as a result of the higher dV_{ce}/dt, a higher surge I_c is induced due to the larger reverse recovery current from the FWD. The high surge currents of TCIGBT can be effectively suppressed by replacing the silicon PiN diodes with the silicon carbide (SiC) Schottky diodes, which will be evidenced in the later analysis.

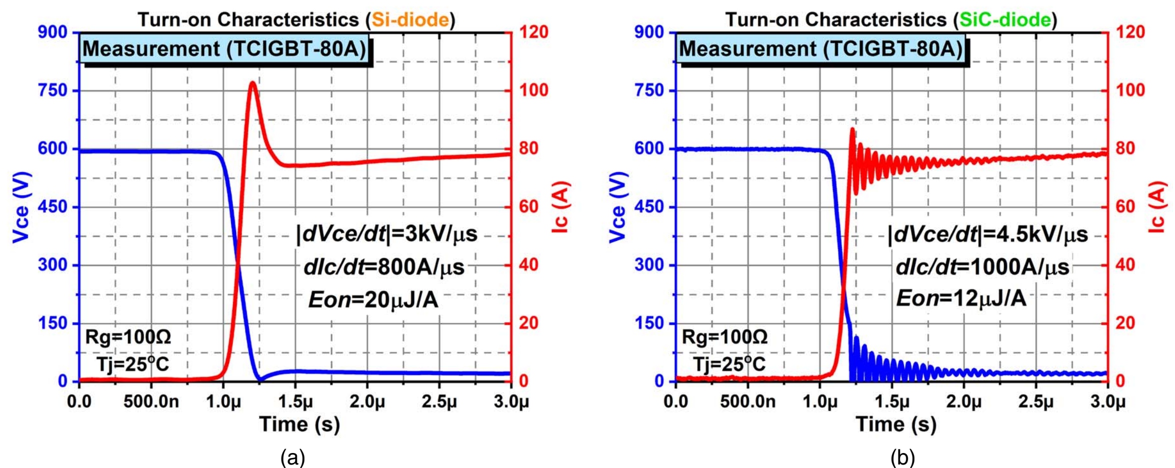

Fig. 5. (Color online) Measured turn-on performance of (a) TCIGBT with silicon diode and (b) TCIGBT with SiC diode. ($V_g - V_{th} = \pm 10$ V; $T_j = 25$ °C).

© 2022 The Author(s). Published on behalf of The Japan Society of Applied Physics by IOP Publishing Ltd

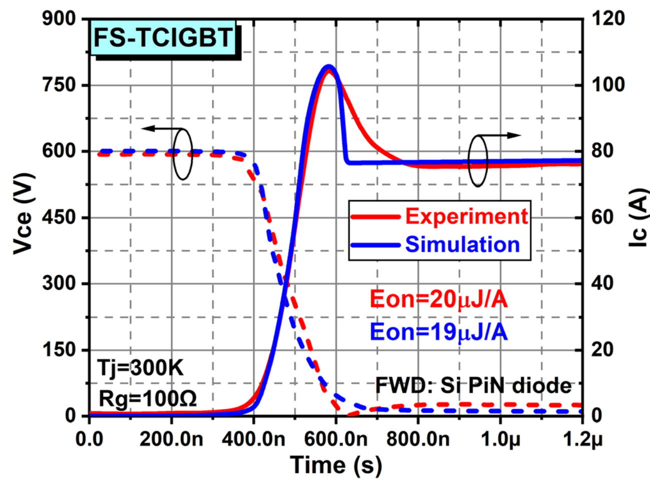

Fig. 6. (Color online) Comparison of measured turn-on waveforms and simulated turn-on waveforms of FS-TCIGBT.

To confirm the low E_{on} performance of TCIGBT and analyze the impact of FWD on the turn-on performance, the turn-on behavior of a 1.2 kV 80 A ($J_c = 175$ A cm^{-2}) TCIGBT in field-stop (FS) technology is characterized through experiments, as shown in Figs. 5(a) and 5(b). Both a silicon PiN diode[26] and a SiC diode[27] are used as FWD to compare the turn-on performance. It can be seen that the SiC diode reduces the surge current and improves the dV_{ce}/dt in the turn-on transients. Moreover, compared to a state-of-the-art TIGBT device ($E_{on} = 73\ \mu$J A^{-1} at $T_j = 25$ °C),[28] the TCIGBT with silicon diode shows a 73% reduction of E_{on} while the TCIGBT with SiC diode shows an 84% reduction of E_{on}. Therefore, the TCIGBT technology provides a superior solution for improving the turn-on power dissipation of MOS-bipolar power devices.

To verify the consistency between the simulation results and measurement results, Fig. 6 compares the measured turn-on waveforms and the simulated turn-on waveforms of a calibrated TCIGBT model. It can be seen that the simulated waveforms are close to the measured results.

In addition to the low E_{on} performance, the TCIGBT design can suppress the NGC effect in the turn-on transients due to the self-clamping feature. The physics of the NGC effect can be explained as follows. In the conventional TIGBT, the hole current flows into the P-float region and evacuates along the trench sidewall. The P-float potential (V_{PF}), as shown in Fig. 7, is therefore raised during turn-on. If the voltage difference across the gate oxide (V_{PF}–V_{ge}) is high, a reverse displacement current will be induced to charge the gate capacitance to a negative value, which has a significant impact on the dV_{ce}/dt and dI_c/dt controllability.[19] Figure 8 compares the V_{PF} and the V_{ge} of TIGBT and TCIGBT during turn-on transients. It can be seen that there is a significant potential difference between V_{PF} and V_{ge} in the TIGBT, which is caused by the hole current flow within the P-float region. However, in the case of TCIGBT, the floating P-base potential is clamped under a low value due to the self-clamping feature and the N-well acts as a barrier for the holes. Therefore, the hole current is evacuated through the mesa region directly via the PMOS structure formed by the p$^+$-cathode/N-well/P-well, as shown in Fig. 7. Hence, the potential difference across the gate oxide is marginal and the NGC effect is therefore successfully suppressed.

3. Impact of scaling rules on turn-on performance

Figures 9(a) and 9(b) show the scaling concepts on TIGBT[1] and TCIGBT,[4] respectively. The structural parameters are identical to the values in Refs. 1 and 4. Figures 10(a) and 10(b) compare the turn-on waveforms and V_{PF} during turn-on transients between k1-TIGBT and k3-TIGBT, respectively. As shown, the gate charge (Q_g) is scaled in k3-TIGBT due to the scaled trench gates. However, the NGC effect is enhanced in the $k3$-TIGBT due to the IE effect. Figures 11 and 12 show the dV_{ce}/dt and the dI_c/dt of TIGBTs and TCIGBTs, respectively. It can be seen that the dV_{ce}/dt and the dI_c/dt of both k3-TIGBT and k3-TCIGBT are increased compared to that of conventional structures. Hence, the scaling rules result in a significant reduction of E_{on} in both TIGBT and TCIGBT, as shown in Fig. 13. Due to the enhanced thyristor effect,[4] k3-TCIGBT shows the lowest E_{on} in this comparison. The turn-on dI_c/dt controllability with respect to the E_{on} is shown in Fig. 14. As the NGC effect is enhanced by the scaling rules in TIGBT, the dI_c/dt-E_{on} trade-off of the k3-TIGBT is degraded compared to that of k1-TIGBT. In contrast, in the TCIGBT, E_{on} can be reduced by the scaling

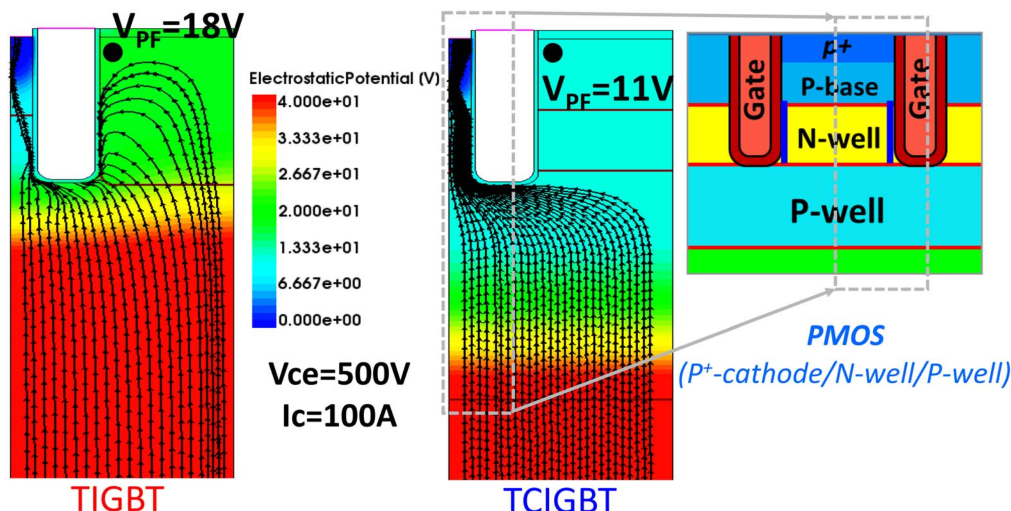

Fig. 7. (Color online) Comparison of current flowlines and potential distribution during turn-on of TIGBT and TCIGBT at $I_c = 100$ A and $V_{ce} = 500$ V.

© 2022 The Author(s). Published on behalf of The Japan Society of Applied Physics by IOP Publishing Ltd

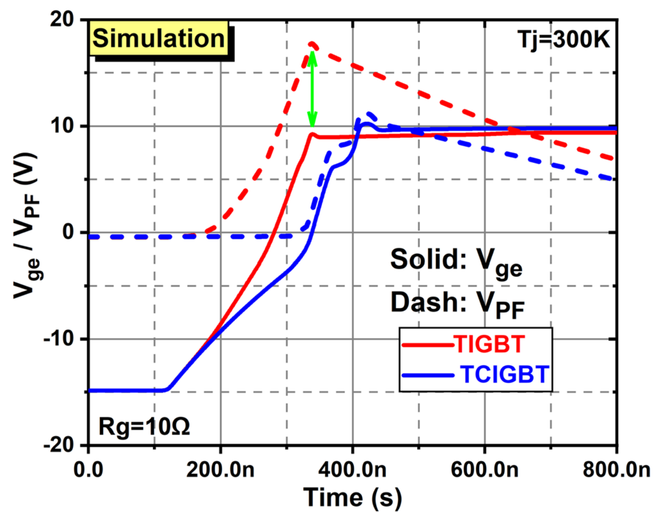

Fig. 8. (Color online) Comparison of turn-on V_{ge} and V_{PF} of TIGBT and TCIGBT at identical R_g.

design as same as the TIGBT. However, the suppression of NGC is kept even in the scaled TCIGBT due to the enhanced self-clamping feature.[4] Therefore, the dI_c/dt-E_{on} trade-off of the TCIGBT is slightly improved by the scaling design. At $dI/dt = 5$ kA μs^{-1}, $k3$-TCIGBT shows a 70% reduction of E_{on} compared to that of $k3$-TIGBT.

4. High current density operation

The continuous increase in power density is important for the development of power semiconductor devices to achieve low cost and design optimization for power electronic systems. Higher power densities require reliable operations at higher operating current densities with low energy loss per chip area. However, it is found that the DA phenomenon limits the reduction of E_{off} of conventional TIGBT and scaled TIGBTs.[9] Moreover, experimental results confirm that the DA phenomenon is enhanced at high current density operations,[9] which limits the maximum operating current density and affects the long-term reliability.[5,7] Therefore, the DA must be suppressed or eliminated when increasing the operating current density of the MOS-bipolar power switches. Due to DA-free performance,[8,11] the current density of TCIGBTs can be continuously increased without DA-related concerns. Figure 15 shows the I–V and current saturation characteristics of the fabricated 1.2 kV

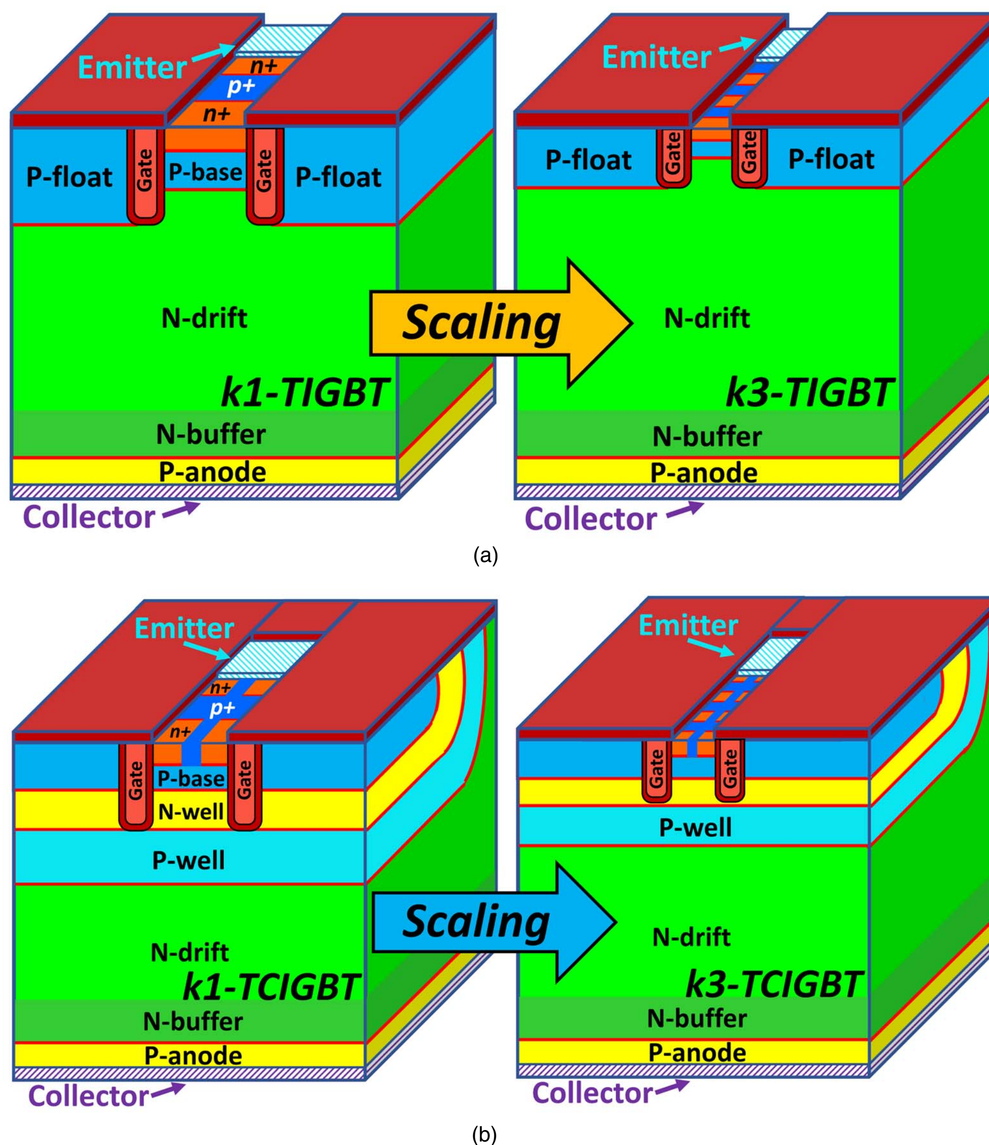

Fig. 9. (Color online) 3D scaling concepts on (a) TIGBT and (b) TCIGBT.

© 2022 The Author(s). Published on behalf of The Japan Society of Applied Physics by IOP Publishing Ltd

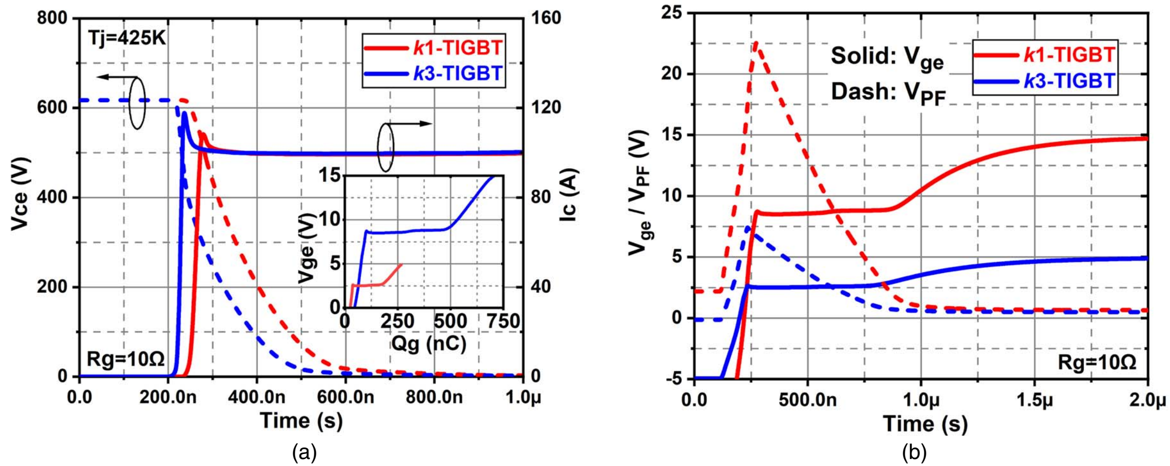

Fig. 10. (Color online) Comparison of (a) turn-on waveforms and (b) V_{ge} and V_{PF} during turn-on transients of k1-TIGBT and k3-TIGBT.

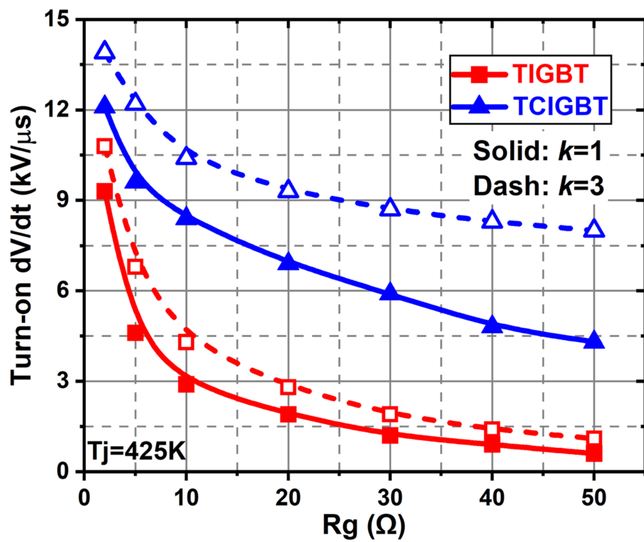

Fig. 11. (Color online) Comparison of turn-on dV_{ce}/dt of scaled TIGBTs and scaled TCIGBTs.

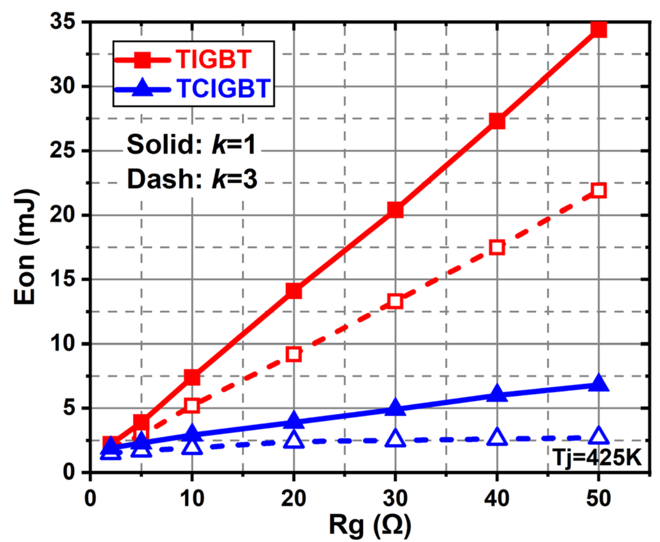

Fig. 13. (Color online) Comparison of E_{on} of scaled TIGBTs and scaled TCIGBTs.

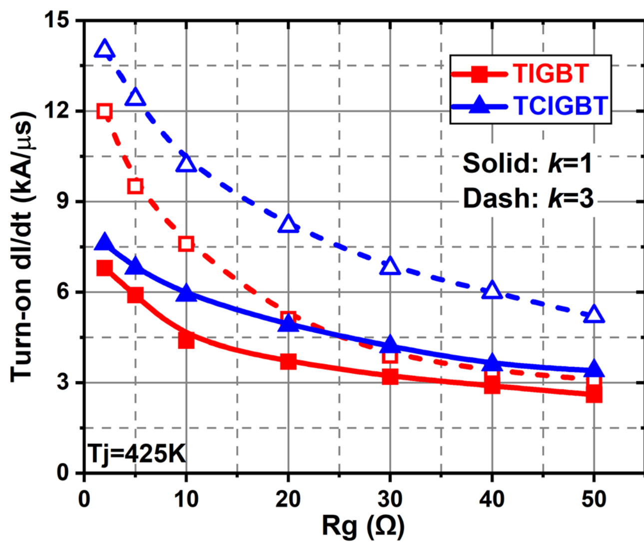

Fig. 12. (Color online) Comparison of turn-on dI_c/dt of scaled TIGBTs and scaled TCIGBTs.

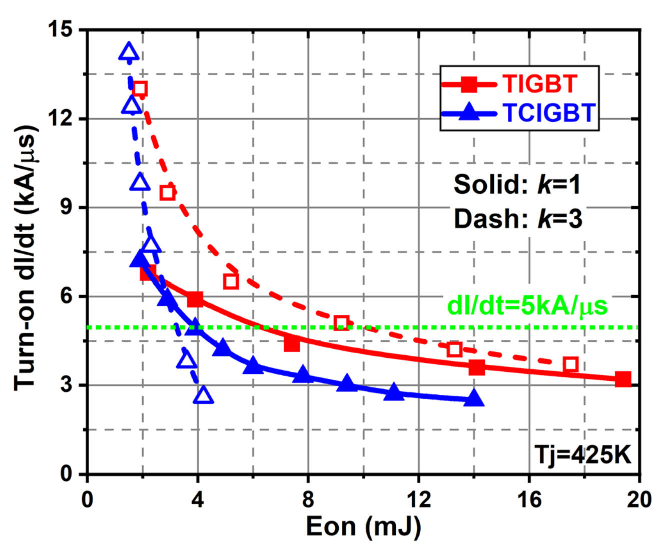

Fig. 14. (Color online) Comparison of dI_c/dt-E_{on} trade-off of scaled TIGBTs and scaled TCIGBTs.

© 2022 The Author(s). Published on behalf of The Japan Society of Applied Physics by IOP Publishing Ltd

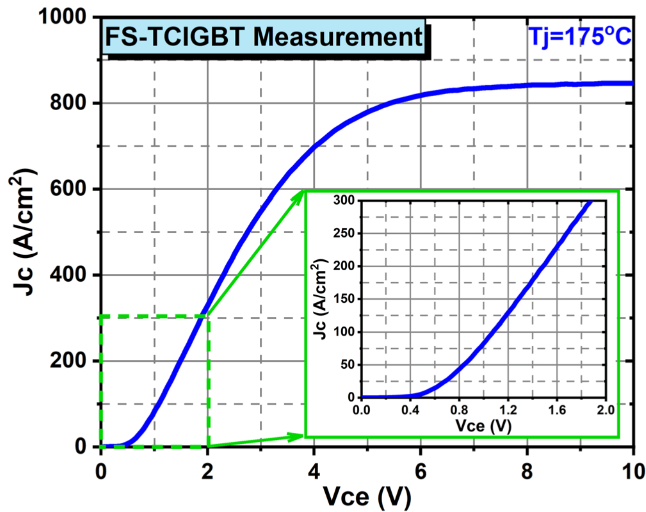

Fig. 15. (Color online) Measured *I–V* and current saturation characteristics of 1.2 kV FS-TCIGBT at $T_j = 175$ °C.

FS-TCIGBT at $T_j = 175$ °C. It can be seen that the FS-TCIGBT shows a low $V_{ce(sat)}$ of 1.87 V at $J_c = 300$ A cm^{-2} and $T_j = 175$ °C as well as a low current saturation level due to the self-clamping feature. Figures 16(a) and 16(b) show the measurement results of the impact of current density on the total power loss of FS-TCIGBT at $T_j = 25$ °C and $T_j = 175$ °C, respectively. A commercial FS-TIGBT[28] is used as a benchmark and the power losses are calculated at $I_c = 100$ A and identical maximum dV_{ce}/dt conditions. As the P-anode dose of TCIGBT has not been optimized, the turn-off loss of TCIGBT is higher than that of TIGBT, but the on-state losses at different current densities are lower than that of TIGBT. Therefore, it can be seen that the FS-TCIGBT shows much lower power losses than the benchmark FS-TIGBT. For example, an 18% reduction of total power loss can be achieved by the FS-TCIGBT operated at $J_c = 300$ A cm^{-2} and $T_j = 175$ °C. In addition, the FS-TCIGBT does not show a significant increase in total power losses with the increase in operating current density. Therefore, the FS-TCIGBT is well suited for high current density operations with low energy losses and DA-free performance.

Figures 17(a) and 17(b) compares the total power loss of scaled TIGBTs and scaled TCIGBTs at $J_c = 200$ A cm^{-2} and $J_c = 500$ A cm^{-2}, respectively. The E_{on} and E_{off} are calculated at the minimum R_g that can achieve DA free. As shown, scaling rules result in a 10% reduction of total power loss in both TIGBTs and TCIGBTs. *k*3-TCIGBT shows a 40% reduction of total power loss compared to *k*3-TIGBT at

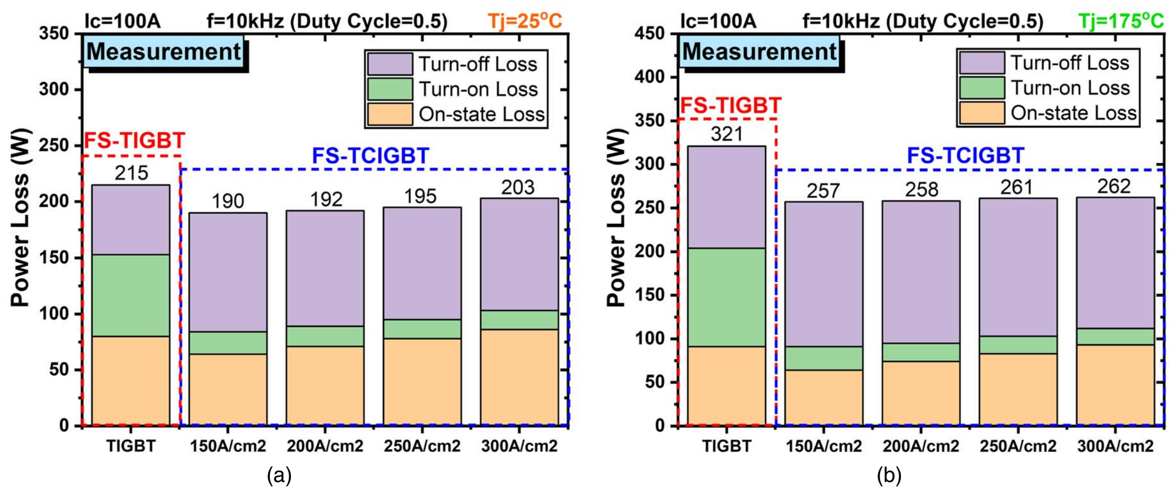

Fig. 16. (Color online) Impact of current density on the total power loss of FS-TCIGBT at (a) $T_j = 25$ °C and (b) $T_j = 175$ °C.

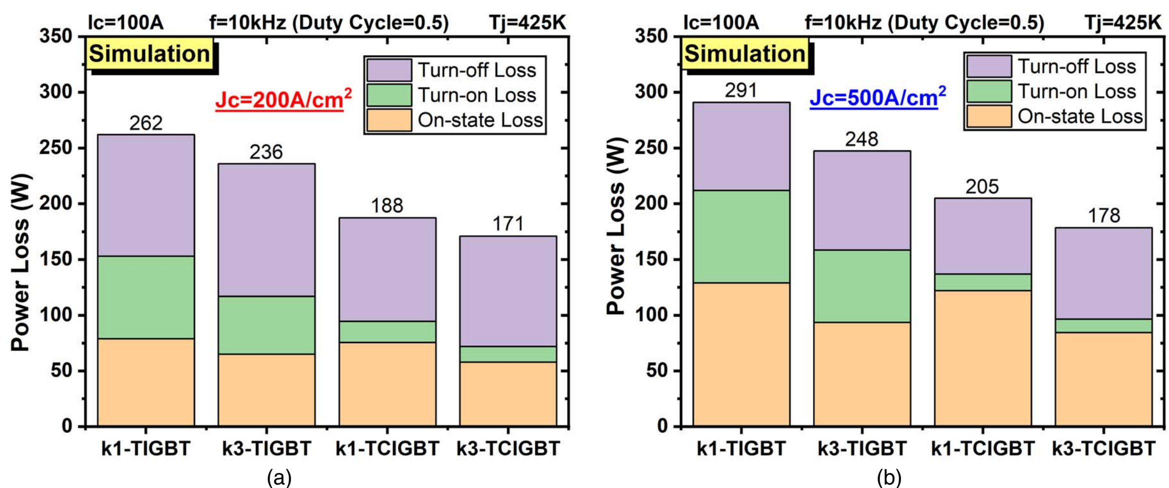

Fig. 17. (Color online) Comparison of total power loss of scaled TIGBTs and scaled TCIGBTs at (a) $J_c = 200$ A cm^{-2} and (b) $J_c = 500$ A cm^{-2}.

© 2022 The Author(s). Published on behalf of The Japan Society of Applied Physics by IOP Publishing Ltd

$T_j = 425$ K. Therefore, the energy efficiency of TCIGBTs can be further improved by the employment of 3D scaling rules.

5. Conclusions

The turn-on behavior of TIGBT and TCIGBT are studied using TCAD simulations as well as experiments. The E_{on} is significantly reduced in TCIGBT due to higher current gain and the negative gate capacitance effect is effectively suppressed by the self-clamping feature. Moreover, the scaling rules on TIGBT and TCIGBT result in a significant reduction of E_{on}. The k3-TCIGBT shows high power efficiency due to the enhanced thyristor effect as well as DA-free performance. Finally, experimental results show that TCIGBT shows an 18% reduction of total power loss compared to the state-of-the-art TIGBT even when operated at $J_c = 300$ A cm^{-2} and $T_j = 175$ °C.

Acknowledgments

The authors would like to acknowledge Eco Semiconductors Ltd for the supply of 1.2 kV FS-TCIGBT samples.

1) K. Kakushima et al., "Experimental verification of a 3D scaling principle for low $V_{ce(sat)}$ IGBT," IEDM Tech. Dig., 2016, p. 10.6.1.
2) T. Saraya et al., "Demonstration of 1200V scaled IGBTs driven by 5V gate voltage with superiorly low switching loss," IEDM Tech. Dig., 2018, p. 8.4.1.
3) T. Saraya et al., "Impact of structural parameter scaling on on-state voltage in 1200 V scaled IGBTs," Jpn. J. Appl. Phys. **59**, SGGD18 (2020).
4) P. Luo, H. Y. Long, M. R. Sweet, M. M. D. Souza, and E. M. S. Narayanan, "Numerical analysis of 3D scaling rules on a 1.2-kV trench clustered IGBT," IEEE Trans. Electron Devices **65**, 1440 (2018).
5) J. Lutz and R. Baburske, "Dynamic avalanche in bipolar power devices," Microelectron. Reliab. **52**, 475 (2012).
6) S. Machida, K. Ito, and Y. Yamashita, "Approaching the limit of switching loss reduction in Si-IGBTs," Proc. 26th Int. Symp. Power Semiconductor Devices and IC's (ISPSD), 2014, p. 107.
7) T. Laska, F. Hille, F. Pfirsch, R. Jereb, and M. Bassler, "Long term stability and drift phenomena of different trench IGBT structures under repetitive switching tests," Proc. 19th Int. Symp. Power Semiconductor Devices and IC's (ISPSD), 2007, p. 1.
8) P. Luo, E. M. S. Narayanan, S. Nishizawa, and W. Saito, "Dynamic avalanche free design in 1.2kV Si-IGBTs for ultra high current density operation," IEDM Tech. Dig., 2019, p. 12.3.1.
9) P. Luo, S. N. E. Madathil, S. I. Nishizawa, and W. Saito, "Evaluation of dynamic avalanche performance in 1.2-kV MOS-bipolar devices," IEEE Trans. Electron Devices **67**, 3691 (2020).
10) P. Luo, S. N. E. Madathil, S. I. Nishizawa, and W. Saito, "'Turn-OFF *dV/dt* controllability in 1.2-kV MOS-bipolar devices,'," IEEE Trans. Power Electron. **36**, 3304 (2021).
11) P. Luo, S. N. E. Madathil, and P. D. Souza, "Experimental demonstration of a 1.2-kV trench clustered insulated gate bipolar transistor in field-stop technology," 2021 IEEE 12th Energy Conversion Congress & Exposition - Asia (ECCE-Asia), 2021, p. 1319.
12) M. Shiraishi, T. Furukawa, S. Watanabe, T. Arai, and M. Mori, "Side gate HiGT with low *dv/dt* noise and low loss," Proc. 28th Int. Symp. Power Semiconductor Devices and IC's (ISPSD), 2016, p. 199.
13) K. Ohi, Y. Ikura, A. Yoshimoto, K. Sugimura, Y. Onozawa, H. Takahashi, and M. Otsuki, "Ultra low Miller capacitance trench-gate IGBT with the split gate structure," Proc. 27th Int. Symp. Power Semiconductor Devices and IC's (ISPSD), 2015, p. 25.
14) M. Sawada, K. Ohi, Y. Ikura, Y. Onozawa, M. Otsuki, and Y. Nabetani, "Trench shielded gate concept for improved switching performance with the low Miller capacitance," Proc. 28th Int. Symp. Power Semiconductor Devices and IC's (ISPSD), 2016, p. 207.
15) K. Matsushita, H. Ninomiya, T. Naijo, M. Izumi, and S. Umekawa, "Low gate capacitance IEGT with trench shield emitter (IEGT-TSE) realizing high frequency operation," Proc. 25th Int. Symp. Power Semiconductor Devices and IC's (ISPSD), 2013, p. 269.
16) F. Wolter, W. Roesner, M. Cotorogea, T. Geinzer, M. Seider-Schmidt, and K. Wang, "Multi-dimensional trade-off considerations of the 750 V micro pattern trench IGBT for electric drive train applications," Proc. 27th Int. Symp. Power Semiconductor Devices and IC's (ISPSD), 2015, p. 105.
17) T. Ogura, H. Ninomiya, K. Sugiyama, and T. Inoue, "Turn-off switching analysis considering dynamic avalanche effect for low turn-off loss high-voltage IGBTs," IEEE Trans. Electron Devices **51**, 629 (2004).
18) I. Omura, W. Fichtner, and H. Ohashi, "Oscillation effects in IGBT's related to negative capacitance phenomena," IEEE Trans. Electron Devices **46**, 237 (1999).
19) Y. Onozawa, M. Otsuki, N. Iwamuro, S. Miyashita, T. Miyasaka, Y. Seki, and T. Matsumoto, "1200-V low-loss IGBT module With low noise characteristics and high *dI/dt* controllability," IEEE Trans. Ind. Appl. **43**, 513.
20) Y. Toyota et al., "Novel 3.3-kV advanced trench HiGT with low loss and low *dv/dt* noise," Proc. 25th Int. Symp. Power Semiconductor Devices and IC's (ISPSD), 2013, p. 29.
21) M. Sawada, Y. Sakurai, K. Ohi, Y. Ikura, Y. Onozawa, T. Yamazaki, and Y. Nabetani, "Hole path concept for low switching loss and low EMI noise with high IE-effect," Proc. 29th Int. Symp. Power Semiconductor Devices and IC's (ISPSD), 2017, p. 65.
22) S. Watanabe, M. Mori, T. Arai, K. Ishibashi, Y. Toyoda, T. Oda, T. Harada, and K. Saito, "1.7 kV trench IGBT with deep and separate floating p-layer designed for low loss, low EMI noise, and high reliability," Proc. 23rd Int. Symp. Power Semiconductor Devices and IC's (ISPSD), 2011, p. 48.
23) P. Luo, S. N. E. Madathil, W. Saito, and S. I. Nishizawa, "Performance comparison of scaled IGBTs and CIGBTs," 2021 Int. Conf. on Solid State Devices and Materials (SSDM), 2021.
24) I. Synopsys, 09Sentaurus Device User Guide: Version R02020.09.
25) M. Sweet, O. Pulber, J. V. S. C. Bose, L. Ngwendson, K. V. Vershinin, M. M. D. Souza, and E. M. S. Narayanan, "Clustered insulated gate bipolar transistor: a new power semiconductor device," IEE Proc. - Circuits, Devices and Systems, 2001, Vol. 148, p. 75.
26) (Datasheet: IXYS Diode HiPerFRED: DSEP60-12AR [Online]).
27) (Datasheet: CREE Silicon Carbide Schottky Diode: C4D30120D [Online]).
28) (Datasheet: Infineon EasyPIM module with Trenchstop IGBT 7 and Emitter Controlled 7 diode and PressFIT/NTC: FP10R12W1T7_B11 [Online]).

© 2022 The Author(s). Published on behalf of The Japan Society of Applied Physics by IOP Publishing Ltd